


RESEARCH

Open Access



Repopulating Kupffer cells originate directly from hematopoietic stem cells

Xu Fan^{1,2}, Pei Lu², Xiang-Hua Cui², Peng Wu¹, Wei-Ran Lin¹, Dong Zhang³, Shong-Zong Yuan⁴, Bing Liu⁵, Fang-Yan Chen¹, Hong You², Han-Dong Wei¹, Fu-Chu He^{1,6*}, Ji-Dong Jia^{2*} and Ying Jiang^{1,7*} 

Abstract

Background Kupffer cells (KCs) originate from yolk-sac progenitors before birth. Throughout adulthood, they self-maintain independently from the input of circulating monocytes (MOs) at a steady state and are replenished within 2 weeks after having been depleted, but the origin of repopulating KCs in adults remains unclear. The current paradigm dictates that repopulating KCs originate from preexisting KCs or monocytes, but there remains a lack of fate-mapping evidence.

Methods We first traced the fate of preexisting KCs and that of monocytic cells with tissue-resident macrophage-specific and monocytic cell-specific fate-mapping mouse models, respectively. Secondly, we performed genetic lineage tracing to determine the type of progenitor cells involved in response to KC-depletion in mice. Finally, we traced the fate of hematopoietic stem cells (HSCs) in an HSC-specific fate-mapping mouse model, in the context of chronic liver inflammation induced by repeated carbon tetrachloride treatment.

Results By using fate-mapping mouse models, we found no evidence that repopulating KCs originate from preexisting KCs or MOs and found that in response to KC-depletion, HSCs proliferated in the bone marrow, mobilized into the blood, adoptively transferred into the liver and differentiated into KCs. Then, in the chronic liver inflammation context, we confirmed that repopulating KCs originated directly from HSCs.

Conclusion Taken together, these findings provided *in vivo* fate-mapping evidence that repopulating KCs originate directly from HSCs, which presents a completely novel understanding of the cellular origin of repopulating KCs and shedding light on the divergent roles of KCs in liver homeostasis and diseases.

Keywords Kupffer cells, Repopulation, Genetic inducible fate-mapping, Progenitor cells, Hematopoietic stem cells, Proliferation, Differentiation, Chronic liver inflammation, Monocytic cells, Self-maintain

*Correspondence:

Fu-Chu He

hefc@bmi.ac.cn

Ji-Dong Jia

jia_jd@cmmu.edu.cn

Ying Jiang

jiangying304@hotmail.com

¹ State Key Laboratory of Medical Proteomics, Beijing Proteome Research Center, National Center of Protein Sciences (Beijing), Beijing Institute of Lifeomics, Beijing 102206, China

² Liver Research Center, Beijing Friendship Hospital, Capital Medical University, Beijing Key Laboratory of Translational Medicine in Liver Cirrhosis and National Clinical Research Center of Digestive Diseases, Beijing 100050, China

³ Research Center, Beijing Friendship Hospital, Capital Medical University, Beijing Key Laboratory of Tolerance Induction and Organ Protection in Transplantation, Beijing 10050, China

⁴ Department of Lymphoma, Fifth Medical Center of Chinese PLA General Hospital, Beijing 100071, China

⁵ State Key Laboratory of Experimental Hematology, Fifth Medical Center of Chinese PLA General Hospital, Beijing 100071, China

⁶ Research Unit of Proteomics Driven Cancer Precision Medicine, Chinese Academy of Medical Sciences, Beijing 102206, China

⁷ Anhui Medical University, Hefei 230032, China



© The Author(s) 2023. **Open Access** This article is licensed under a Creative Commons Attribution 4.0 International License, which permits use, sharing, adaptation, distribution and reproduction in any medium or format, as long as you give appropriate credit to the original author(s) and the source, provide a link to the Creative Commons licence, and indicate if changes were made. The images or other third party material in this article are included in the article's Creative Commons licence, unless indicated otherwise in a credit line to the material. If material is not included in the article's Creative Commons licence and your intended use is not permitted by statutory regulation or exceeds the permitted use, you will need to obtain permission directly from the copyright holder. To view a copy of this licence, visit <http://creativecommons.org/licenses/by/4.0/>. The Creative Commons Public Domain Dedication waiver (<http://creativecommons.org/publicdomain/zero/1.0/>) applies to the data made available in this article, unless otherwise stated in a credit line to the data.

Introduction

Kupffer cells (KCs), the tissue-resident macrophages (TRMs) in the liver, play crucial roles in liver homeostasis and in the pathogenesis of liver diseases [1]. According to the common mononuclear phagocyte system theory, all TRMs including KCs originate from and are continuously replenished by circulating MOs [2]. However, the concept has been being undermined by the new insight that the majority of TRMs including KCs originate from yolk-sac erythro-myeloid progenitors [3]. Furthermore, unlike skin and intestine, the adult liver resists the colonization of monocyte-derived macrophages and retains fetal-derived KCs with the potential of long-term self-maintaining [4, 5], at a steady state.

Previous studies showed KCs are replenished within two weeks even following a severe depletion [6]. However, the cellular origin of repopulating KCs remains unclear. It has been suggested that preexisting KCs [3, 7] or MOs [8, 9] were the cellular origins of repopulating KCs. The former hypothesis is mainly supported by the findings that repopulation of KCs is independent of the signal of CC chemokine receptor 2 (CCR2), a chemokine receptor predominantly expressed on monocytes [5], that KCs have the potential of proliferation *in vitro* upon inactivation of transcription factors MafB and c-Maf [10], and that KCs proliferate actively in context of glucan-induced granuloma formation [11]. The second hypothesis is mainly supported by the findings that a partial replacement of KCs by bone marrow (BM)-derived progenitors is observed in BM transplantation experiments [12], in adoptive transfer experiments [9], and in severe experimental *Listeria* infection [13]. However, both of these hypotheses have yet to be confirmed by *in vivo* fate-mapping evidence.

Therefore, the purpose of the current study was to determine whether repopulating KCs originate from pre-existing KCs or from MOs, as previously reported, using genetic inducible fate-mapping and, if not, to determine what type of progenitor cells give rise to repopulating KCs. For this purpose, we first traced the fate of pre-existing KCs and that of MOs during KC-repopulation, in a TRM- and a monocyte-specific genetic inducible fate-mapping mouse model, we found no evidence that repopulating KCs originate from preexisting KCs or from MOs. Then, using genetic lineage tracing we found that hematopoietic stem cells (HSCs) act as progenitor cells in response to KC-depletion. Finally, employing an HSC-specific fate-mapping system, we confirmed that repopulating KCs originate directly from HSCs, in the context of chronic liver inflammation induced by repeated carbon tetrachloride (CCl₄) treatment, a commonly used mouse model associated with KC-depletion without MO-depletion.

Materials and methods

Mice strains and procedures

Tg(Csf1r-Mer-iCre-Mer)1Jwp mice (Jax#019098), R26R-EYFP mice (Jax#006148), W/Wv mice (Jax#100410), mT/mG mice (Jax#007676), Cx3cr1^{<tm2.1(cre/ERT2)Jung>/J} mice (Jax#020940), Fgd5^{ZsGr.CreERT2} mice (Jax#027789), B6 ACTb-EGFP mice (Jax#003291) were purchased from the Jackson Laboratory. Stop-Cas9 mice (#T002249) were purchased from NanJing Biomedical Research Institute of Nanjing University (China). Wild-type C57BL/6 mice were obtained from the Institute of Laboratory Animal Science Chinese Academy of Medical Science. CCR2-mice (Jax#004999) were kindly provided by Dr. Li Tang (Beijing Institute of Lifeomics). Unless otherwise stated, mice were used at 6–12 weeks of age. Experimental mice were age- and sex-matched.

The investigators were blinded to the genotype of the animals during the experimental procedure. All experiments included littermate controls. Embryonic development was estimated considering the day of vaginal plug formation as 0.5 days post-coitum (DPC). All mice were bred and maintained in specific pathogen-free facilities at the National Center of Protein Sciences (Beijing). All experimental protocols were approved by the Institutional Animal Care and Use Committee of National Center of Protein Sciences (Beijing) and were conducted in accordance with ethical regulations (Approval no. IACUC-20151221-12). The reporting of the animal experiments conforms to the ARRIVE guideline (<https://arriveguidelines.org/arrive-guidelines>). Reagents were from Sigma-Aldrich (Poole, UK) unless otherwise specified.

PCR genotyping of FVB-Tg^{(Csf1r-cre/Esr1*)1Jwp/J}, B6.129X1-Gt(ROSA)26Sor^{tm1(EYFP)Cos/J}, WBB6F1/J-Kitw/Kitw-v/J, B6.129(Cg)-Gt(ROSA)26Sor^{tm4(ACTB-tdTomato,-EGFP)} Luo, B6.129P2(C)-Cx3cr1^{<tm2.1(cre/ERT2)Jung>/J}, C57BL/6N-Fgd5^{tm3(cre/ERT2)Djr/J}, and C57BL/6-Tg^{(CAG-EGFP)10sb/J} mice, B6-Gt(ROSA)26Sor^{tm1(CAG-LSL-cas9,-tdTomato)/Nju} mice, and B6.129^{S4-Ccr2tm1lfc/J} mice was performed according to the manufacturer's instructions.

Pulse labeling of Csf1r⁺ progenitors in embryos, Cx3cr1⁺ monocytic cells and Fgd5⁺ HSCs in adults

For genetic cell labeling of Csf1r⁺ progenitors in embryos, mice embryos recombination was induced by a single injection of 75 µg/g (body weight) of tamoxifen (Sigma, T-5648) into pregnant females. To counteract the mixed estrogen agonist effects of tamoxifen, which can result in late fetal abortions, progesterone (Sigma, P-3972) dissolved in sterile vegetable oil was added for IP injections into pregnant females.

For genetic cell labeling Cx3cr1⁺ monocytic cells and Fgd5⁺ HSCs in adults, adult-mice recombination was

induced by a 5-day consecutive injection of 200 $\mu\text{g/g}$ (body weight) of tamoxifen.

Isolation of cells from the blood, bone marrow, and liver

Blood cells were collected as previously described [14] before analysis by flow cytometry. Briefly, each mouse was humanely restrained in a modified plastic tube, exposing one of the hind limbs. The hair was removed using electric clippers, and a thin layer of petroleum jelly was applied to the skin. The saphenous vein was punctured using a sterile 4 mm lancet, and blood was collected into a microvette tube containing 2 mg/ml EDTA.

Bone marrow cells were collected as previously described [15] before analysis by flow cytometry. Briefly, killed mice were immersed in 75% ethanol. The skin was clipped mid-back and removed from the lower part of the body. The tissue was removed from the legs with scissors and dissected away from the body. Each end of the bone was cut off, and, using a 27 g needle/1 ml syringe filled with PBS, the bone marrow was expelled from both ends of the bone with a jet of medium directed into a 15 ml cell culture dish. The cell suspension was filtered through a 70- μm filter mesh to remove any bone spicules or muscle and cell clumps.

Non-parenchymal liver cells were isolated as described previously [16]. In short, the liver was perfused with collagenase and incubated at 25 °C for 10 min in DNase I solution. After collagenase digestion was halted with 5 mM EDTA solution, the resulting single-cell suspension was subjected to velocity and density centrifugation in an iodixanol gradient (Axis-Shield, Oslo, Norway) to produce purified suspensions of non-parenchymal cells.

Flow cytometry

Erythrocytes in the blood were lysed using FACS^{lyse} solution (BD Pharmingen, San Diego, CA). The isolated cells were surface stained in FACS buffer (PBS w/o Ca^{2+} Mg^{2+} supplemented with 0.5% BSA and 5 mM EDTA) for 30 min on ice. Multi-parameter analysis and flow cytometric cell sorting were performed on a FACS Aria II (BD Biosciences San Jose, CA) and analyzed with FlowJo software (Tree Star, Inc., Ashland, OR, USA).

For absolute F4/80⁺ cell counts, total NPCs isolated from each mouse were stained and sorted separately, and the cell number was counted with flow cytometry during FACS. Fluorochrome-conjugated mAbs specific to mouse F4/80 (clone BM8), CD115 (clone AFS98), Ly6C (HK 1.4), Ly6A/E (clone D7), CD117 (clone 2B8), CD135 (clone A2F10), CD34 (clone SA376A4), CD207 (clone 4C7), I-A/I-E (clone M5/114.15.2), and the corresponding isotype controls were purchased from BioLegend (San Diego, CA, USA.). CD3e (clone 145-2c11), CD19 (clone 1D3), and a lineage cocktail with an isotype

control (561317) and the Annexin/PE Apoptosis Detection Kit I were purchased from BD Pharmingen (San Diego, CA). The gating strategies of KCs, BM HSCs macrophages, and blood leukocytes are shown in Additional file 1: Fig. S10.

Transplantation of HSCs without irradiation

HSC transplantation in non-irradiated Kit^{W/W^v} mice was performed as described previously. In brief, approximately 2000 HSCs (Lin^{neg} Sca-1⁺ c-kit⁺, CD34⁻ CD135⁻) isolated from the bone marrow of 3-week-old B6GFP mice, which carry a constitutively active EGFP reporter allele, were injected into 16-week-old Kit^{W/W^v} mice. Recipients were analyzed 8 weeks after transplantation for donor/host chimerism in bone marrow, blood, and liver.

Kupffer cell depletion with clodronate liposomes

1:1 PBS-diluted clodronate liposomes (Clo) and control liposomes (FormuMax Scientific, Palo Alto CA, USA) were injected via the intraperitoneal as 20 mg/kg or 10 mg/kg.

An experimental model of liver injury

Acute liver injury: Mice received 0.6 mL/kg body weight of CCl₄ mixed with corn oil intraperitoneally and were killed at the indicated time points.

Chronic liver injury: CCl₄ was injected twice weekly for 6 weeks. Mice were killed at the indicated time point after the last injection.

At indicated time points after liver injury, mice were euthanized using carbon dioxide (CO₂) in accordance with the NIH Guidelines for the euthanasia of animals, with minimal stress to them. Briefly, a cage containing 3–5 mice was placed in a separate 20-L volume chamber. Compressed 99.99% CO₂ gas in a cylinder was connected to and introduced into the chamber with a flow rate of 10 L per minute. The mice were all unconsciousness in 3 min, lacking spontaneous breathing. After another minute's CO₂ flow, the mice were checked again to confirm with no respiration, their eye color faded, and no pupillary response to light. The mice were then removed from the cage, and the liver tissues were harvested. After liver injury, mice were only excluded/euthanized humanely in time when the animal health condition was poor.

Magnetic enrichment of lineage cells from single-cell suspension of bone marrow

Depletion of lineage-committed cells from single-cell suspensions of mouse bone marrow was performed using the EasySep[™] Mouse Hematopoietic Progenitor Cell Isolation Kit according to the manufacturer's instructions (StemCell Technologies, Vancouver, BC, Canada).

Labeling DNA of proliferating cells with 5-ethynyl-2'-deoxyuridine in vivo

Incorporation of 5-ethynyl-2'-deoxyuridine (Edu) was measured using the Click-iT Edu flow cytometry assay kit according to the manufacturer's instructions (Life technologies, Carlsbad, CA, USA). Briefly, Edu was dissolved in DMSO at 25.5 mg/ml and further diluted in PBS to 5 mg/ml. Mice were injected i.v. with 50 µg/g Edu 1 day prior to kill. Controls received DMSO/PBS.

Histopathological examination

Each formaldehyde-fixed sample was embedded in paraffin, cut into 5-µm-thick sections, and stained with hematoxylin-eosin (H-E) according to standard procedures. All slides were reviewed by the same pathologist.

Cell transfer

Sorted populations isolated from the bone marrow of every clodronate-liposome-treated, B6GFP⁺ donor mouse at 5 days post-clodronate-liposome injection (HSCs, 3.0×10^4 cells per mouse; multipotent progenitors (MPPs), 3.0×10^4 cells per mouse and MOs, 5.0×10^5 cells per mouse) were injected intravenously into each clodronate-liposome-treated C57BL/6 mice at 5 days post-clodronate-liposome injection.

Statistical analysis

Results represent the mean ± s.e.m. unless otherwise indicated. Statistical significance was determined as indicated in figure legends. Statistical analyses were done with Prism GraphPad software v5.0, and the exact tests used are indicated within the appropriate text.

Results

Repopulating KCs did not originate from preexisting KCs

Given that adult mouse TRMs originate from colony-stimulating factor 1 receptor (Csf1r)-expressing yolk-sac progenitors [17], an inducible Csf1r^{MeriCreMer} fate-mapping system is widely used for labeling Csf1r-expressing yolk-sac progenitors and to follow their progeny in adult mice [18]. Accordingly, we traced the fate of preexisting KCs during KC-repopulation as follows.

Csf1r^{CreERT2} activity was induced with a pulse of tamoxifen in Csf1r^{MeriCreMer}; Rosa^{mT/mG} mouse embryos at E8.5. To selectively deplete KCs without depleting bone marrow macrophages (Additional file 1: Fig. S1A, B), and without triggering liver inflammation (Additional file 1: Fig. S1C, D), 20 mg/kg of Clo was intraperitoneally injected into pulsed mice 8 weeks after birth. To determine the contribution of "non-KCs" to KC-repopulation, we compared the KC-labeling index before and after KC-repopulation. The rationale for this approach was as follows: If repopulating KCs originate from genetically

labeled preexisting KCs, then the KC-labeling index should remain unchanged. In contrast, if repopulating KCs originate from unlabeled progenitor cells, then the KC-labeling index should decrease [19].

To label KCs, a tamoxifen pulse at E8.5 resulted in labeling that was completely restricted to KCs and did not extend to HSCs or blood leukocytes (Fig. 1A). No labeled KCs were detected in tamoxifen-treated Csf1r^{wt}; Rosa^{mT/mG} animals (No Cre) (Fig. 1C). Furthermore, no differences were observed in the labeling indexes of the MHCII⁺ or MHCII⁻ KC-subgroups [20] or the CD68⁺ or CD68⁻ KC-subgroups [21] (Fig. 1B and Additional file 1: Fig. S2A), indicating that the labeling was not restricted to a specific KC-subgroup.

After complete repopulation following 90% KC-depletion (10–90 days post-Clo injection), the mean KC-labeling index for the clodronate liposomes group (repopulation after depletion) was reduced by approximately 95% compared with the control-liposomes group (no depletion) [0.14 ± 0.06 vs. $5.42 \pm 1.44\%$] (Fig. 1C, D). The proliferative ability of KCs might be impaired because of their near-complete depletion. To exclude this possibility, only 60% of KCs were depleted by intraperitoneal injection of 10 mg/kg clodronate liposomes in 8-week-old Csf1r^{MeriCreMer}; Rosa^{mT/mG} mice (Additional file 1: Fig. S2B, C), pulsed with tamoxifen at E8.5. Similarly, the mean KC-labeling index for the clodronate liposomes group was reduced by 70% compared with the control-liposomes group [1.79 ± 0.69 vs. $5.41 \pm 1.62\%$] (Fig. 1E, F). Moreover, we found that the KC-labeling index remained unchanged through 90 days post KC-repopulation.

Furthermore, we compared the percentage of 5-ethynyl-2'-deoxyuridine (Edu) positive labeled/unlabeled KCs from mice at different time points post-Clo injection. We found that there are no Edu positive labeled/unlabeled KCs in mice till 10-day post-Clo injection (Additional file 1: Fig. S3). These results indicated that both labeled and unlabeled KCs have no differential proliferation potential.

Together, these results demonstrated that repopulating KCs do not originate from genetically labeled GFP⁺ pre-existing KCs.

Repopulating KCs originated from hematopoietic progenitors (HPs) in bone marrow

Next, we attempted to determine what type of progenitor cells give rise to repopulating KCs. Previous studies demonstrate that some KCs are of donor hematopoietic progenitor origin in BM chimeras [12]. However, such transplantation protocols do not accurately reflect KC-repopulation under physiological conditions. In particular, that protocol involved total-body

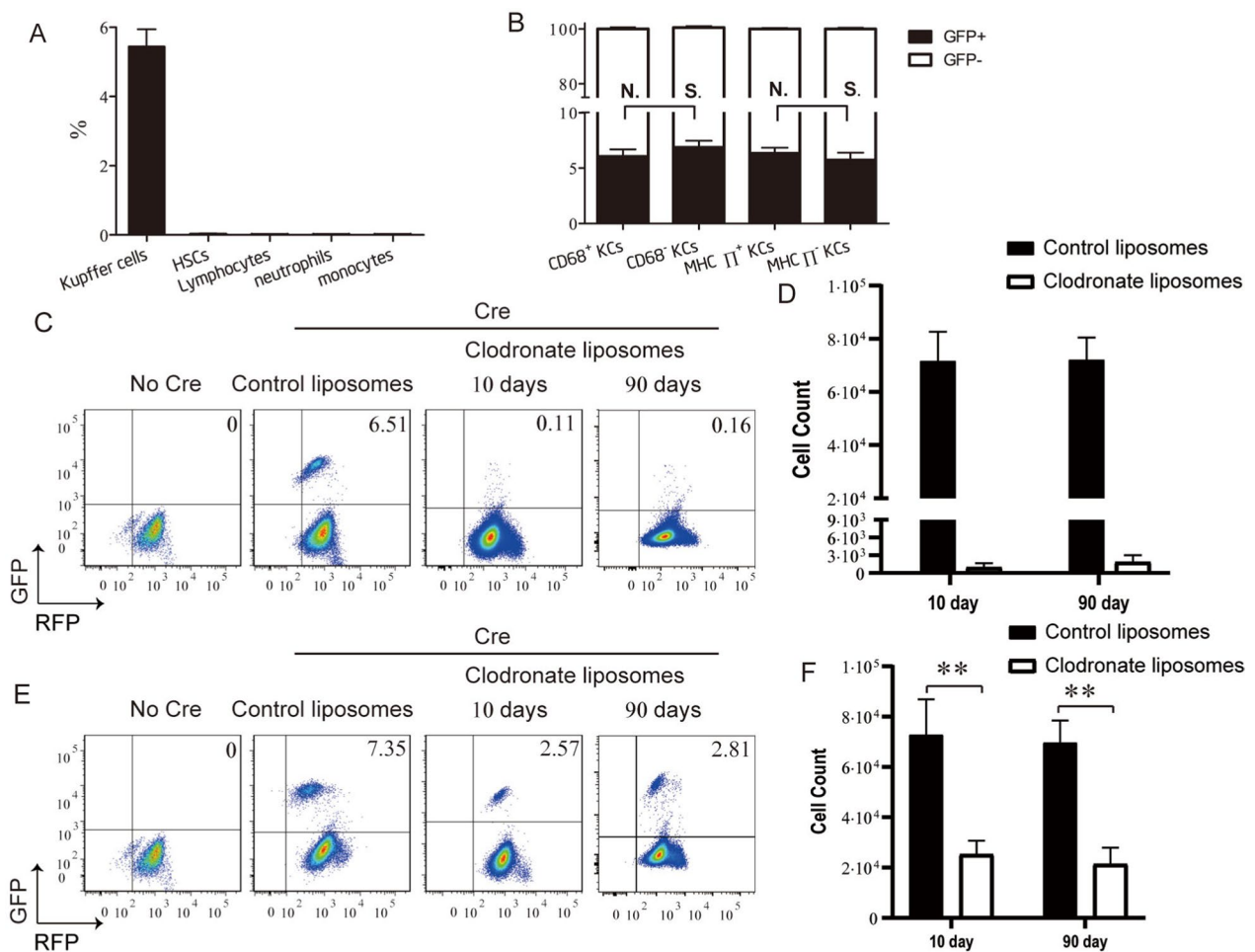


Fig. 1 Repopulating kupffer cells (KCs) do not originate from preexisting KCs. **A** Label index of KCs, hematopoietic stem cells (HSCs), lymphocytes, neutrophils, and monocytes from E8.5-pulsed $Csf1r^{MerCreMer}; Rosa^{mT/mG}$ mice (Cre mice). Values are the means \pm SEM from 6 samples. **B** Label index of $CD68^+$ or $CD68^-$, and $MHCII^+$ or $MHCII^-$ KC-subgroups from Cre mice. Values are the means \pm SEM from 6 samples. N.S. No significant difference between indicated groups by t test. **C** Flow cytometric analysis of KCs from E8.5-pulsed $Csf1r^{Wt}; Rosa^{mT/mG}$ mice (No Cre mice) or from Cre mice at 10 day and 90 day post-intraperitoneal injection (i.p.) with 20 mg/kg of control-liposomes or 20 mg/kg of clodronate liposomes. **D** Cell counts of KCs from indicated mice analyzed in C. Values are the means \pm SEM from 6 samples. $***P < 0.001$ between groups by t test. **E** Flow cytometric analysis of KCs from No Cre mice or from Cre mice at 10 day and 90 day post-i.p. with 10 mg/kg of control-liposomes or 10 mg/kg of clodronate liposomes. **F** Cell counts of KCs from indicated mice analyzed in E. Values are the means \pm SEM from 6 samples. $**P < 0.01$ between groups by t test

irradiation, which could affect peripheral cell entry into the liver by impairing the integrity of the hepatic sinusoid [7]. Therefore, we traced the fate of hematopoietic progenitors during KC-repopulation under physiological conditions as follows. Purified HSCs (defined as $Lin^{neg}Sca-1^+c-kit^+CD34^-CD135^-CD48^-CD150^+$) from B6GFP transgenic mice were engrafted into Kit^W/Kit^{WV} recipients, which can accept HSC grafts in the C57BL/6 background without myeloablation [22].

To selectively deplete KCs by approximately 90% or 60%, 20 mg/kg or 10 mg/kg of Clo were intraperitoneally injected into HSCs chimeras, respectively, at 8 weeks

post-engraftment. To determine whether hematopoietic progenitors contribute to KC-repopulation, the total number of host-origin KCs after depletion and after complete repopulation was compared. The rationale for this approach was that if repopulating KCs originate from donor-origin hematopoietic progenitors, then the total number of host-origin KCs should remain unchanged throughout repopulation.

We found that 8 weeks after engraftment, only hematopoietic cells (including HSCs, MOs, neutrophils, and most lymphocytes) not KCs within the recipients were of donor HSC origin (Fig. 2A, B and Additional file 1:

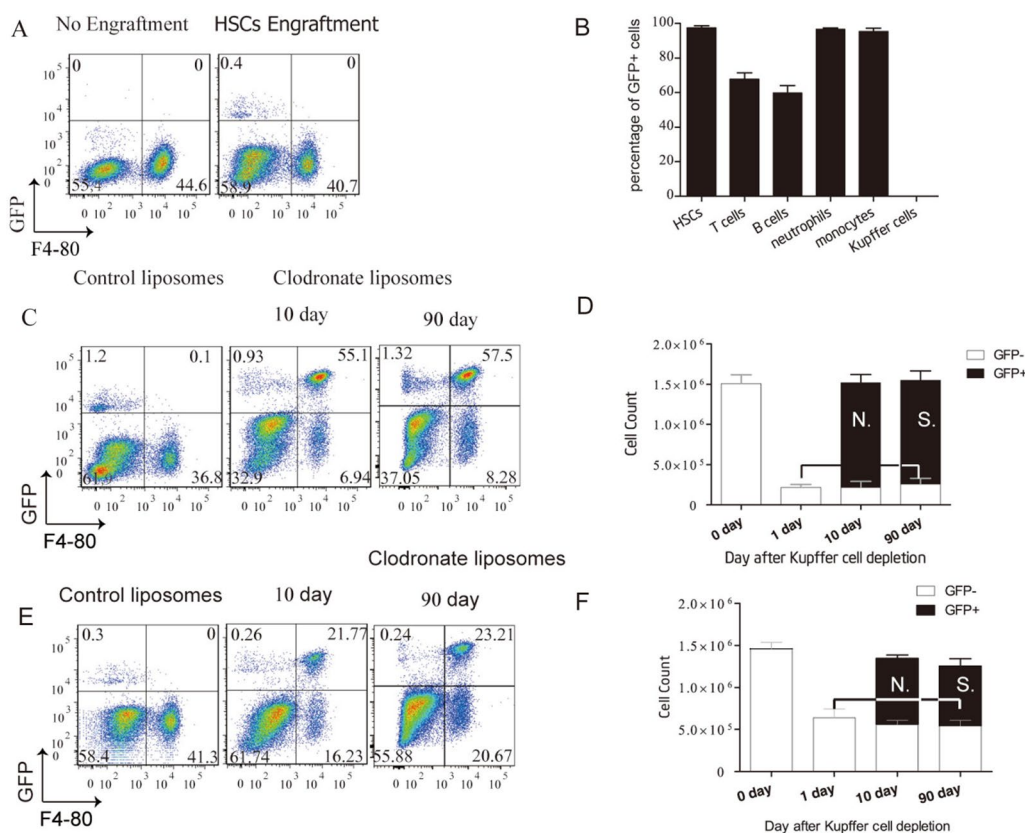


Fig. 2 Repopulating kupffer cells (KCs) originate from hematopoietic progenitors. **A** Flow cytometric analysis of liver non-parenchymal cells from purified GFP⁺ hematopoietic stem cell (HSC)-chimeric Kit^W/Kit^{WV} mice before engraftment (no engraftment) and 8 week post-enugraftment (HSC-enugraftment). **B** Donor chimerism of HSCs, T-cells, B-cells, neutrophils, monocytes, and KCs from HSC-chimeric Kit^W/Kit^{WV} mice analyzed in A. Values are the means ± SEM from 3 samples. **C** Flow cytometric analysis of liver non-parenchymal cells from HSC-chimeric Kit^W/Kit^{WV} mice at 10 and 90 day post-intraperitoneal injection (i.p.) with 20 mg/kg of clodronate liposomes (90% KC-depletion). **D** Cell counts of KCs from HSC-chimeric Kit^W/Kit^{WV} mice at 0, 1, 10, and 90 day after 90% KC-depletion. Values are the means ± SEM from 4 samples N.S., no significant difference between groups by ANOVA. **E** Flow cytometric analysis of liver non-parenchymal cells from HSC-chimeric Kit^W/Kit^{WV} mice at 10 and 90 day post-i.p. with 10 mg/kg of clodronate liposomes (60% KC-depletion). **F** Cell counts of KCs from HSC-chimeric Kit^W/Kit^{WV} mice at 0, 1, 10 and 90 day after 60% KC-depletion. Values are the means ± SEM from 4 samples N.S., no significant difference between groups by ANOVA

Fig. S4). For the observation period from 10 to 90 days post-Clo injection (0 days and 80 days post-complete KC repopulation), all repopulating KCs were labeled with GFP (Fig. 2C–F). These results demonstrated that all repopulating KCs originate from hematopoietic progenitors in the BM.

Repopulating KCs did not originate from MOs

We then sought to test the hypothesis that repopulating KCs originate from MOs. For this purpose, we induced Cre activity by Tamoxifen administration in adult Cx3cr1^{CreERT2}; Rosa^{YFP} mice [23] and then dynamically investigated the labeling index of MOs. We found that during an observation period of 2–25 days after 5 days of consecutive tamoxifen administration, Cx3cr1^{CreERT2}; Rosa^{YFP} mice showed labeling in all MOs, including macrophages and DC progenitors (MDPs), common monocyte progenitors (cMoPs), MOs in BM, Ly6C^{hi} or Ly6C^{low}

MOs in the blood (Additional file 1: Fig. S4A), and intra-splenic MOs (Additional file 1: Fig. S5B, C). However, almost all HSCs and KCs were unlabeled (Additional file 1: Fig. S5D). As expected, no labeled MOs were detected in tamoxifen-treated Cx3cr1^{wt}; Rosa^{YFP} animals (Additional file 1: Fig. S5E).

Thus, we traced the fate of circulating MOs and of intra-splenic MOs during KC-repopulation as follows. To label MOs, adult Cx3cr1^{CreERT2}; Rosa^{YFP} mice were pulsed for 5 days of consecutive of tamoxifen administration. A 15-day wash-out period was conducted to allow tamoxifen levels to dissipate before the initiation of KC-depletion [24]. To determine whether MOs contributed to KC-repopulation, the labeling index ratio of KCs to both Ly6C^{hi} and Ly6C^{low} circulating MOs and the labeling index of KCs to intra-splenic MOs were compared to a constant value (0.9) at 10 days post-clodronate-liposomes injection.

The rationale for this approach was as follows: Following complete repopulation after 90% KC-depletion, if repopulating KCs originate from either circulating MOs or intra-splenic MOs, then the labeling index ratio of repopulating KCs versus Ly6C^{hi} or low MOs should be close to 0.9. However, if repopulating KCs do not originate from MOs and do not express the Cx3cr1 promoter during differentiation, then the KC- labeling index should be close to zero. Finally, if repopulating KCs do

not originate from MOs but do express from the Cx3cr1 promoter during differentiation, and if low levels of Cre activity persist for 3 half-lives [25] (15 days) after tamoxifen administration, then both ratios should be less than 0.9.

We found that throughout KC-repopulation (from 4 to 10 days post-Clo injection), both the label index ratio of KCs versus circulating MOs and the labeling index ratio of KCs vs intra-splenic MOs were less than 0.9 (Fig. 3,

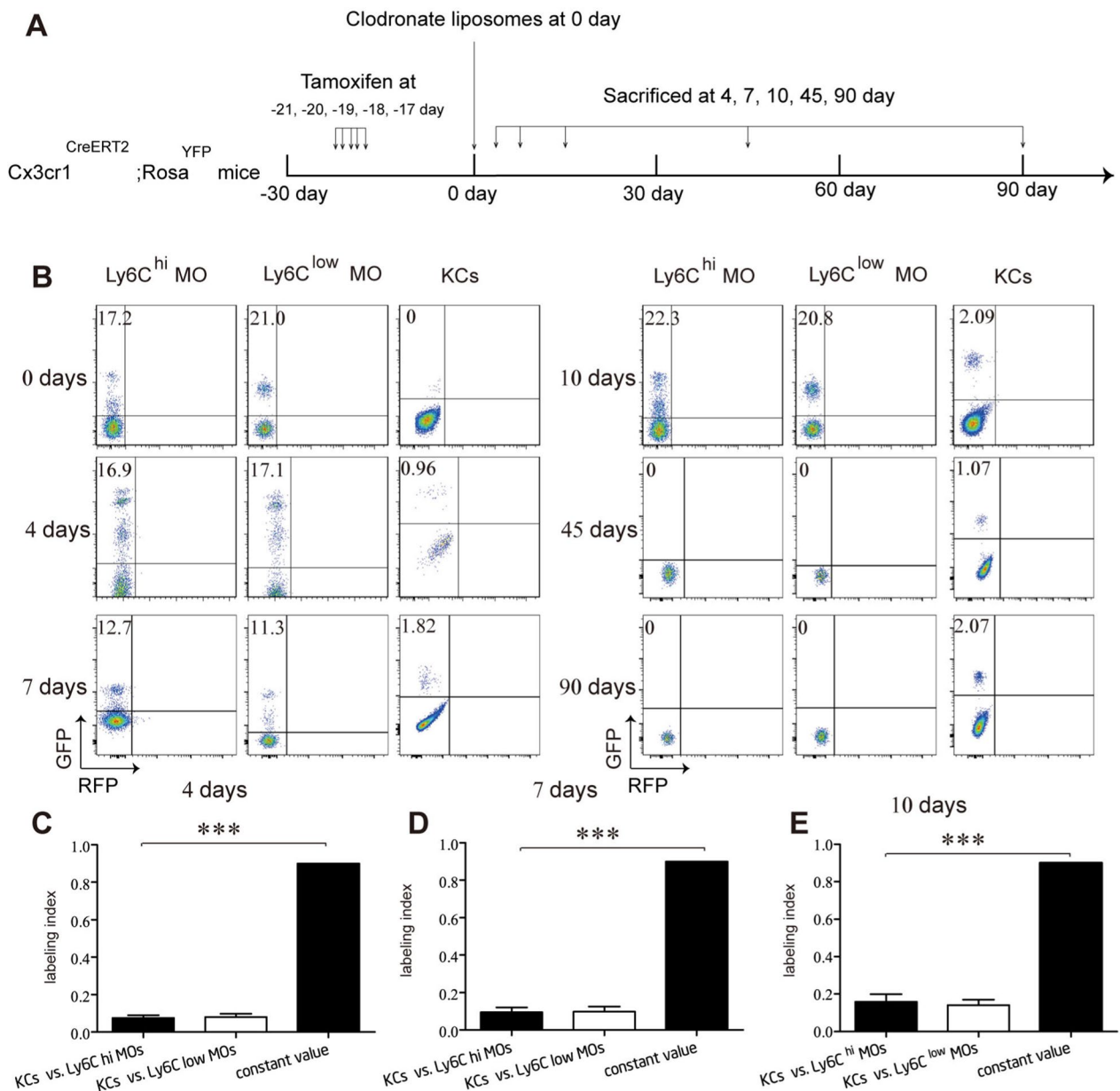


Fig. 3 Repopulating kupffer cells do not originate from MOs. **A** Experimental schedule. **B** Flow cytometric analysis of indicated cells from adult-pulsed Cx3cr1^{CreERT2}; RosaYFP mice (Cre mice) intraperitoneal injection (i.p.) with 20 mg/ml clodronate liposomes (KC-depletion) at indicated time point post-injection (n = 5/group). **C, D, E** Label index of indicated cells from Cre mice at indicated time point post-i.p. with 20 mg/kg of control-liposomes analyzed in **B**. Values are the means ± SEM from 6 samples. ***P < 0.001 between groups by ANOVA

Additional file 1: Fig. S5F–I). At 45 days and 90 days post-Clo injection, although no labeled MOs were detected (Additional file 1: Fig. S5A), the labeling index of repopulating KCs remained unchanged (Fig. 3B). Taken together, these results demonstrate that repopulating KCs originate from unlabeled non-monocytic hematopoietic progenitors rather than labeled MOs.

Hematopoietic stem cells act as progenitors in response to Kupffer cell depletion

Next, we sought to investigate which type of non-monocytic hematopoietic progenitors give rise to repopulating KCs. According to previous reports [26], the progenitor cells for repopulating KCs should have a context-dependent probability of differentiating into repopulating KCs in response to KC-depletion, which is termed the “progenitor cell response.” Given our results show that repopulating KCs originate from non-monocytic hematopoietic progenitor cells in the BM, the progenitor cell response elicited by KC-depletion is defined here as proliferation in BM, mobilization from BM into circulation, engraftment in the liver, and differentiation into KCs. Then, we sought to investigate that triggered by KC-depletion, which type of non-monocytic hematopoietic progenitor cells proliferate in the BM, mobilize from BM into circulation, engraft in the liver, and differentiate into KCs.

For this purpose, we depleted KCs in C57BL/6 mice by intraperitoneal injection with 20 mg/kg of Clo and tracked the number of HSCs during KC-repopulation. We found that the number of HSCs has dramatically increased at 48 h post-Clo injection (2 days before the start of KC-repopulation), peaked at 192 h, and returned to a normal value at 240 h (Fig. 4A and Additional file 1: Fig. S6). Furthermore, we compared the percentage of 5-ethynyl-2'-deoxyuridine (Edu) positive HSCs from mice at 0 and 48 h post-Clo injection. We found that the percentage of Edu⁺ HSCs in mice from the 48 h post-Clo injection group was 60% greater than that in the 0 h post-Clo injection group (Fig. 4B, C) [34.58 ± 5.19% vs. 10.40 ± 3.51%]. These findings indicated that following KC-depletion, HSCs proliferated in the BM.

Next, we performed time-course analysis of HSC-specific markers on blood cells from mice who received Clo injection. We found that a group of cells that express HSCs specific markers (Lin^{neg}Sca-1⁺c-kit⁺CD34⁻CD135⁻) were detected in the blood for an observation period from 48 to 240 h post-Clo injection (Fig. 4D and Additional file 1: Fig. S7), indicating that HSCs mobilized from the bone marrow into the blood during KC-repopulation.

To investigate whether HSCs engraft in the liver and differentiate into KCs, we performed KC-depletion in

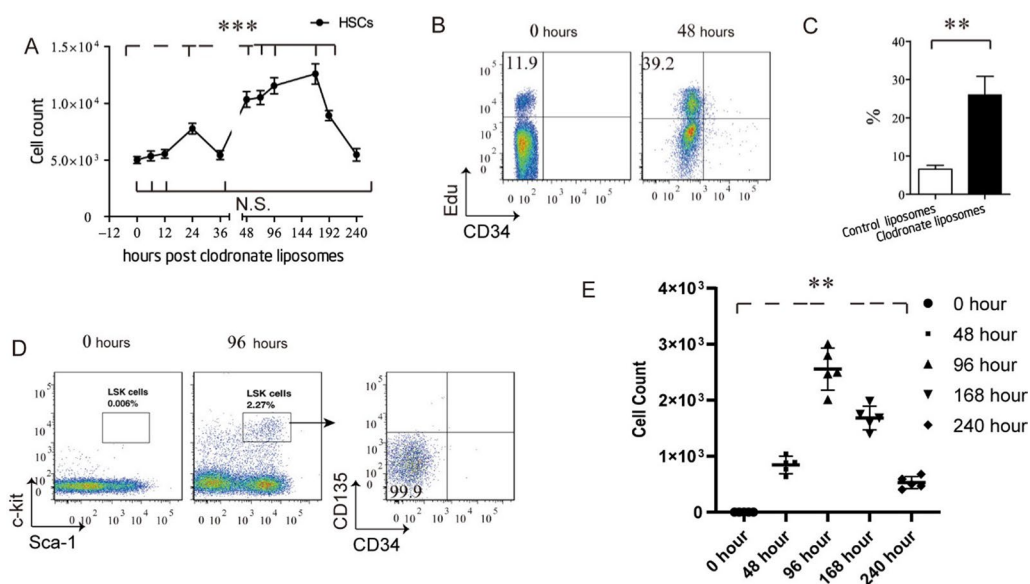


Fig. 4 Hematopoietic stem cells (HSCs) proliferate in the bone marrow and mobilize into the blood, in response to Kupffer cell depletion. **A** Cell count of HSCs from the bone marrow of mice intraperitoneal injection (i.p.) with 20 mg/kg clodronate liposomes at indicated time point post-injection. Values are the means ± SEM from 6 samples. ****P* < 0.001 between groups by ANOVA. **B** flow cytometric analysis of bone marrow hematopoietic progenitors from mice i.p. with 20 mg/kg clodronate liposomes at indicated time point post-injection. **C** Percentage of 5-Ethynyl-2'-deoxyuridine (Edu) ⁺ HSCs from mice i.p. with 20 mg/kg clodronate liposomes at 48 h post-injection. Values are the means ± SEM from 6 samples. ***P* < 0.01 between groups by *t* test. **D** Flow cytometric analysis of blood Lin^{eng} cells from C57BL/6 mice at 4 day after control-liposomes or clodronate liposomes injection. **E** Cell count of blood Lin^{eng} cells from mice i.p. with 20 mg/kg clodronate liposomes at indicated time point post-injection. Values are the means ± SEM from 6 samples. ****P* < 0.01 between groups by ANOVA

both B6GFP and C57BL/6 mice using intraperitoneal injection with 20 mg/k of Clo. Five days post-injection, we engrafted purified HSCs, MPPs (defined as Lin^{neg} Sca-1⁺ C-kit⁺ CD34⁺), or MOs from the BM of Clo-treated B6GFP mice into different Clo-treated C57/BL6 mice (Fig. 5A). Two days post-engraftment, we investigated the expression of HSC-specific markers Sca-1 and c-kit with flow cytometry on donor-origin non-parenchymal liver cells (NPCs) isolated from HSC recipients. We found that Sca-1 and c-kit double-positive cells were detected in donor-origin F4/80⁻ NPCs (Fig. 5B and Additional file 1: Fig. S8), indicating that transferred donor HSCs

adoptively transferred into the liver of the recipient. Then, 10 days post-engraftment, we analyzed the donor-origin marker GFP on F4/80⁺ KCs from HSC, MPP, and monocyte recipients. We found that 4.30 ± 1.36% of F4/80⁺ KCs were GFP positive in the HSC recipients, compared with less than 0.09 ± 0.07% in the MPPs recipients and 0.01 ± 0.005% in the monocyte recipients (Fig. 5C, D), indicating transferred donor HSCs differentiated into KCs following engraftment in the liver of recipients. Finally, 90 days post-engraftment, the donor chimerism of repopulating KCs in recipients remained unchanged (Fig. 5E and Additional file 1: Fig. S9),

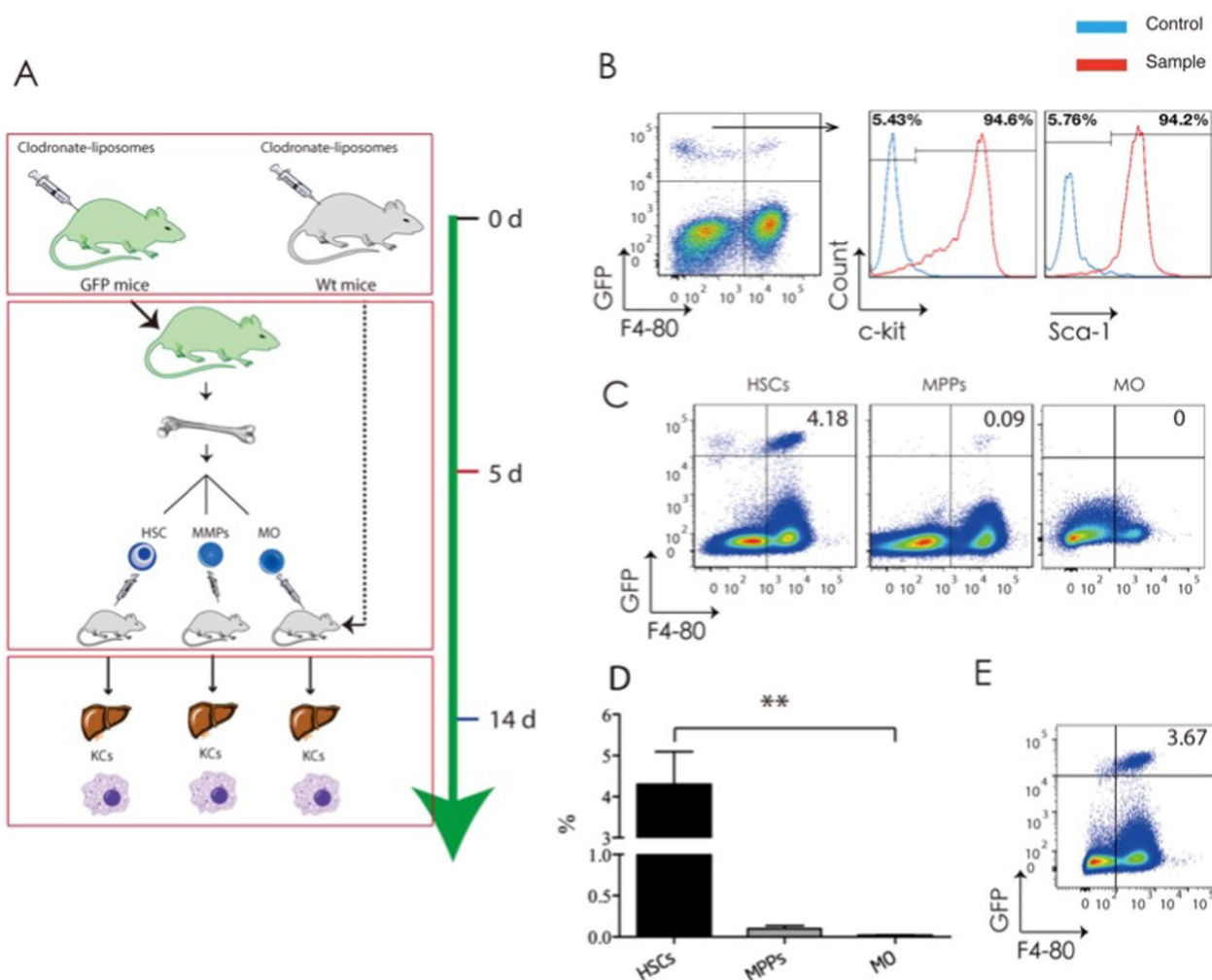


Fig. 5 Hematopoietic stem cells (HSCs) adoptively transfer into the liver and differentiate into Kupffer cells (KCs), in response to KC-depletion. **A** Experimental schedule for adaptive transfer. HSCs are defined as Lin^{neg}Sca-1⁺c-kit⁺CD34⁻CD135⁻CD48⁻CD150⁺ cells, and BM-Mos are defined as Lin^{neg}CD115⁺CD117⁻CD135⁻ cells. **B** Flow cytometric analysis of GFP⁺ donor-origin (sample) or GFP⁻ recipient origin (control) liver non-parenchymal cells (NPCs) from KC-depleted and purified GFP⁺ HSCs-engrafted C57BL/6 mice at 2 day post-engraftment. **C** Flow cytometric analysis of NPCs from KC-depleted and purified GFP⁺ HSCs-engrafted, KC-depleted and purified GFP⁺MPP engrafted, or KC-depleted and purified GFP⁺ MOs (MOs) engrafted C57BL/6 mice at 10-day post-engraftment. **D** Percent of GFP⁺ KCs analyzed in C. Values are the means ± SEM from 6 samples. ***P < 0.001 between groups by ANOVA. **E** Flow cytometric analysis of liver NPCs from KC-depleted or purified GFP⁺ HSCs-engrafted C57BL/6 mice at 90 day post-engraftment

indicating that the repopulating KCs can exist over the long term. Altogether, these data indicated that HSCs act as progenitor cells in response to KC-depletion, including proliferation in the BM, mobilization into the blood, engraftment in the liver, and differentiation into KCs.

Fate-mapping confirmed repopulating KCs originate directly from HSCs

Finally, we used a genetic inducible fate-mapping approach to confirm that repopulating KCs originate directly from HSCs, in a mouse model of chronic liver necro-inflammation induced by CCl₄, in which resident KCs were depleted, while the circulating MOs were not. The depletion of KCs was confirmed by tracking the number of GFP⁻ resident KCs in the liver of non-myeloablative HSC-chimeras treated with repeated CCl₄. We found that the number of resident KCs decreased during repeated CCl₄ and remained at the reduced level for the observation period from 0 till 90-d after cessation of CCl₄ treatment (Fig. 6A–C). We also found a small amount of GFP⁺ macrophages in the liver of HSC chimeras, for the observation period from 14 to 90-d after cessation of CCl₄ treatment, indicating that these cells were resident KCs cells rather than passenger inflammatory macrophages (Fig. 6A–C). In short, these results suggested that during chronic liver inflammation induced by repeated CCl₄ treatment, a small portion of embryonic-derived KCs were depleted and replenished by hematopoietic progenitors.

To further confirm that repopulating KCs originate directly from HSCs, we employed an HSC-specific fate-mapping system constructed by crossing Fgd5-Cre^{ERT2} mice [27] with stop^{tdTomato-Cas9} mice, in which HSCs rather than MOs are genetically labeled. The rationale for this approach is that in this HSC-specific fate-mapping system, the time to reach equilibrium between the labeling index of HSCs and their progeny is especially long because of the exceedingly long residence time of short-term HSCs (ST-HSCs) and of multipotent progenitors [28]. And then, we traced the fate of HSCs during chronic liver inflammation induced by repeated CCl₄ treatment. To label HSCs, Adult Fgd5^{Cre ERT}; ROSA26^{stop-tdTomato-Cas9} mice were pulsed for 5 days of consecutive tamoxifen administration. To deplete KCs, 3 days after the pulse the mice were repeatedly injected with CCl₄. To confirm that repopulating KCs originate directly from HSCs, not from MOs, the labeling index of repopulating KCs, hematopoietic stem and progenitor cells in the BM, and that of peripheral blood leukocytes were detected 21 days after the initiation of CCl₄ treatment. We found that besides HSCs (LT-HSCs) only repopulating KCs were genetically labeled, in the HSC-specific fate-mapping system (Fig. 6D–I). These results indicated that repopulating

KCs originate directly from HSCs, not from MOs or from monocytic progenitors.

Discussion

In this study, in the context of selective KC-depletion induced by Clo or by repeated CCl₄ treatment, we provide in vivo fate-mapping evidence that repopulating KCs originate directly from HSCs, rather than preexisting KCs or MOs.

The long-standing notion that KCs have the potential to proliferate is based largely on measuring DNA-synthesizing KCs that can be labeled with thymidine analogs, in the context of inflammation or granuloma formation [11]. However, it is important to note that these thymidine analogs can be taken by cells undergoing abortive mitosis and by cells repairing DNA [29]. That means incorporation of thymidine analogs does not always mean proliferation of KCs. Most importantly, these studies actually test cell potential instead of cell fate. In our study, the contribution of preexisting KCs to KC-repopulation was excluded by directly tracing the fate of preexisting KCs, a widely used method to determine the extent to which putative progenitor cells contribute to tissue regeneration [30]. In line with this finding, we also demonstrated that all repopulating KCs were of hematopoietic origin in non-myeloablation HSC-chimeras.

A recent lineage-tracing study reported that Ly6C^{hi} monocytes gave rise to repopulating KCs in liver-shielded BM chimeras in which KCs depletion is triggered with diphtheria toxin (DT) administrations [8]. However, it is important to note that inflammatory response triggered by DT administration [31–33] can result in the recruitment of MOs, which can further differentiate into inflammatory macrophages in the liver [34]. Perhaps, that is why the number of Ly6C^{hi} MOs increased in the initial stages of KC repopulation following DT depletion. For the same reason, in DT-treated CCR2^{-/-} KC-DTR recipients, CCR2 expressed donor Ly6C^{hi} MOs were recruited into the liver by MCP-1, and differentiated into inflammatory macrophages which are difficult to be distinguished from KCs.

In the current study, the labeling index of KCs was lower than 10% with adult Csf1r^{MeriCreMer} Rosa26^{YFP} mice pulse-labeled with tamoxifen at E8.5. The commonly low recombination efficiency [17, 35] is due to the low tamoxifen administration dose to overcome the side effects, such as inducing abortion in pregnant mice and perturbing embryonic development [36]. However, the contribution of “non-KCs” to KC-repopulation was determined by comparing the change of the KC-labeling index before and after KC-repopulation, independently from the labeling efficiency.

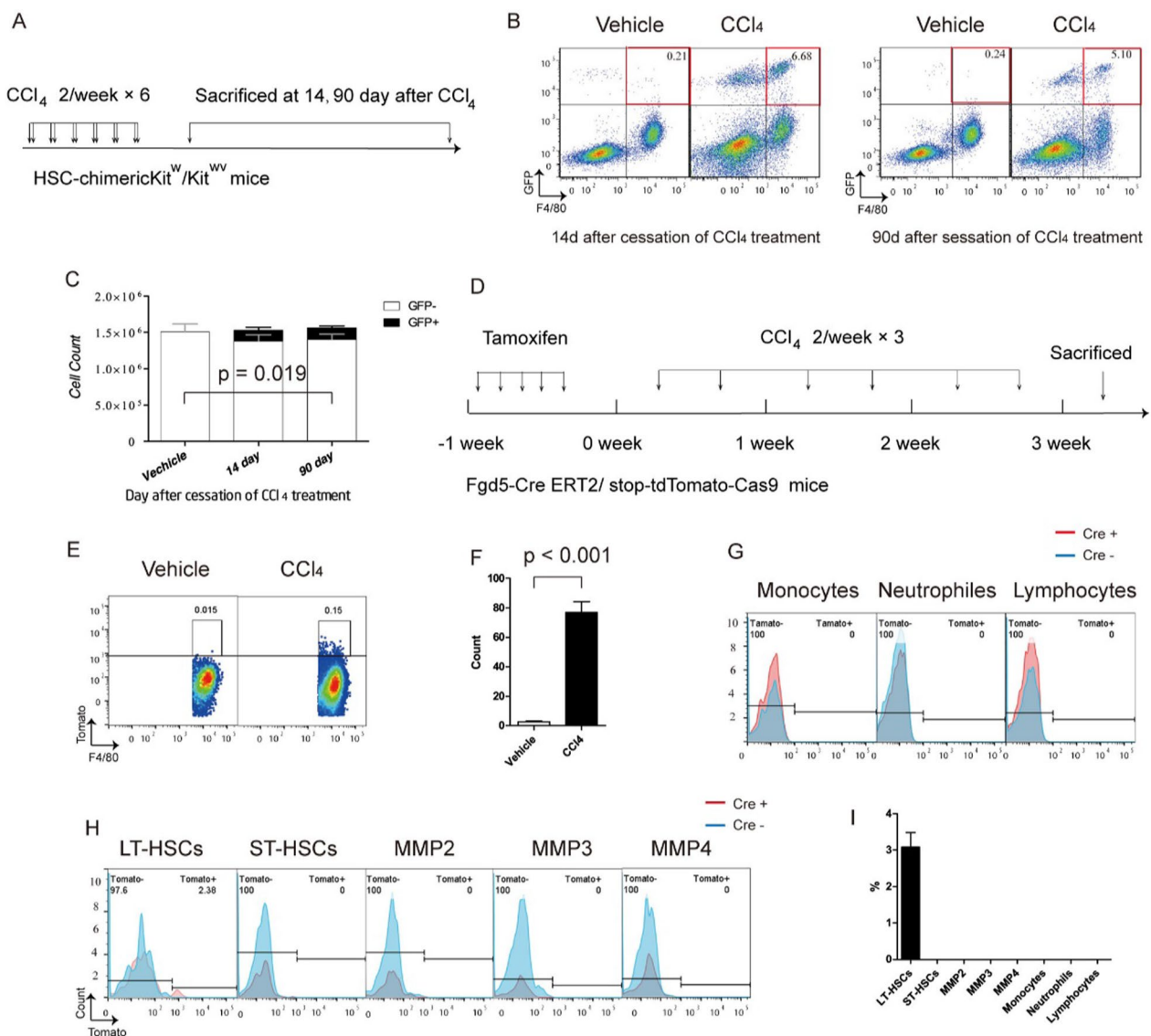


Fig. 6 Repopulating kupffer cells (KCs) originate directly from hematopoietic stem cells (HSCs), in context of CCl₄-induced chronic liver inflammation. **A** Experimental schedule for counting the number of embryonic-derived KCs. **B** Flow cytometric analysis of liver non-parenchymal cells (NPCs) from repeated CCl₄ or vehicle treatment purified GFP⁺ HSC-chimeric Kit^W/Kit^{WV} mice at indicated time point. **C** Cell counts of GFP embryonic-derived KCs from HSC-chimeric Kit^W/Kit^{WV} mice treated with repeated vehicle or CCl₄ at 14 and 90 day after last dose of CCl₄. Values are the means ± SEM from 4 samples analysis by ANOVA. **D** Experimental schedule for tracing the fate of HSCs during Kupffer cell repopulation in the context of chronic liver inflammation induced by repeated CCl₄. **E** Flow cytometric analysis of liver KCs from pulsed Fgd5-Cre ERT2/stop-tdTomato-Cas9 mice received repeated vehicle or CCl₄ treatment at 3-W after first dose vehicle or CCl₄, respectively. **F** Cell count of Tomato⁺ KCs analyzed in **E**. Values are the means ± SEM from 6 samples. ****P* < 0.001 between groups by ANOVA. **G, H** Flow cytometric analysis of hematopoietic stem and progenitors in BM, or peripheral blood leukocytes as indicated from pulsed Fgd5^{Cre ERT2}/stop^{tdTomato-Cas9} mice received repeated vehicle or CCl₄ treatment at 3-W after first dose vehicle or CCl₄, respectively. **I** Percent of Tomato⁺ KCs analyzed in **G** and **H**. Values are the means ± SEM from 6 samples. ****P* < 0.001 between groups by t test

To investigate the repopulation of KCs, not the infiltration of MOs, we first employed a Clo-induced selective KC-depletion approach that did not trigger liver inflammation. Secondly, we employed genetic labeling approaches to distinguish monocyte-derived

inflammatory macrophages from resident KCs, in the context of CCl₄-induced chronic liver inflammation.

We depleted KCs by clodronate liposomes injection, which is a widely used and well-defined model for investigating the function and repopulation of KCs.

Although, similar to the typical limitations found in current models for macrophage depletion, clodronate liposomes injection led to the depletion of a wide array of mononuclear phagocyte cell types, encompassing both bone marrow-derived mononuclear phagocytic system (BM MPS) cells and circulating monocytes [37]. However, in our study, a low dose of clodronate liposomes was injected intraperitoneally (clodronate liposomes is substantially taken up by KCs due to absorption through portal circulation [38]), which selectively depletes KCs but not BM MPS cells. These results indicated that the mobilization of HSCs is a response to KC-depletion, but not a response to depletion of BM MPS cells [39].

In our monocytic cell-specific genetic inducible fate-mapping system, a few repopulating KCs are labeled. One explanation for this finding is that the Cx3cr1 promoter is expressed in the monocytic-intermediate between HSCs and repopulating KCs during differentiation and the residual Cre activity induces gene reconstitution in a few monocytic intermediates, even after a 15-day wash-out period. This presumption is supported by a recent study that reported that although KCs ceased to express the Cx3cr1 chemokine receptor, they obviously originated from Cx3cr1 expressing precursors [23]. The possibility of MOs contributing to KC-repopulation was further excluded by the finding that repopulating KCs are labeled in a HSC-specific fate-mapping system.

Conclusion

In summary, using genetic inducible fate-mapping approaches, we provide strong *in vivo* evidence that repopulating KCs do not originate from preexisting KCs or from MOs, but instead originate directly from HSCs. Our findings may shed light on the divergent roles of KCs in liver homeostasis and diseases. Future studies should consider the mechanism deriving HSC proliferation, migration into the liver, and differentiation into repopulating KCs, including determining the lineage potential of HSCs infiltrated in the liver.

Abbreviations

KCs	Kupffer cells
Mos	Monocytes
HSCs	Hematopoietic stem cells
TRMs	Tissue-resident macrophages
CCR2	CC chemokine receptor 2
BM	Bone marrow
CCl ₄	Carbon tetrachloride
HPs	Hematopoietic progenitors
MDPs	Macrophages and DC progenitors
cMoPs	Common monocytic progenitors
MPPs	Multipotent progenitors

NPCs	Non-parenchymal liver cells
ST-HSCs	Short-term HSCs
DT	Diphtheria toxin
DPC	Days post-coitum
H-E	Hematoxylin–eosin

Supplementary Information

The online version contains supplementary material available at <https://doi.org/10.1186/s13287-023-03569-0>.

Additional file 1. Fig S1. Intraperitoneal injection with 20mg/kg clodronate-liposomes did not deplete bone marrow macrophages and did not trigger liver inflammation. A Flow cytometric analysis of bone marrow-derived mononuclear phagocytic system (BM MPS) cells of C57/BL mice received indicated dose of clodronate-liposomes injection (n = 5/group). B Cell count of BM MPS of C57/BL mice treated with the indicated dose of clodronate-liposomes analyzed in A. C Liver tissue from all normal-saline treatment mice at each time point revealed normal cellular architecture (n = 5). Liver tissue from the clodronate-liposomes group revealed no damage to liver cells and inflammatory cells infiltration (n = 5). Liver tissue from the carbon tetrachloride treatment group revealed some damage to liver cells, inflammatory cells infiltration, fatty changes, and centrilobular necrosis (n = 5), scale bar = 50 μ m. D Serum alanine aminotransferase of mice from the carbon tetrachloride group was significantly increased at 24 hours posttreatment, and returned to normal level at 96 hours (n = 5/group). In contrast, serum alanine aminotransferase of mice from the clodronate-liposomes group and normal saline group was remained unchanged, at the meantime. **Fig S2.** Analysis of kupffer cells (KCs) from C57BL/6 mice following intraperitoneal injection with 20mg/kg clodronate-liposomes. A GFP expression on CD68⁺ and CD68⁻ KCs from E8.5 pulsed Cre mice at 8 weeks after birth. B Flow-cytometric analysis of KCs from C57BL/6 mice 24 hours after being treated with intraperitoneal injection of clodronate-liposomes of indicated dose (n = 6/group). C Percentage of KCs from C57BL/6 mice treated with intraperitoneal injection of clodronate-liposomes of indicated dose analyzed in B. **Fig S3.** Proliferating ratio of bone-marrow-cells (BMCs) and labeled/unlabeled kupffer cells (KCs) from E8.5-pulsed Csf1^{CreERT2}; Rosa^{mT/mG} mice at 10 day and 90 day post-intraperitoneal injection with 20mg/kg of control-liposomes. A Representative results of percentage of EdU⁺ BMCs and labeled/unlabeled KCs. B Percentage of EdU⁺ BMCs or labeled/unlabeled KCs from indicated mice analyzed in A. Values are the means \pm SEM from 6 samples. ***P < 0.001, N.S No significant difference between each Edu/no-Edu group by t-test. **Fig S4.** Flow cytometric analysis of GFP expression of hematopoietic stem cells and blood leukocytes within purified GFP⁺ HSC-chimeric Kitw/Kitw^v mice. **Fig S5.** Flow cytometric analysis of YFP expression of indicated cells within adult pulsed Cx3cr1^{CreERT2}; Rosa^{YFP} mice (Cre) or Cx3^{cr1}^{wt}; Rosa^{YFP} mice (No cre). (A) Flow-cytometric analysis of bone marrow monocytic cells and blood MO from adult pulsed Cx3^{cr1}^{wt}; Rosa^{YFP} or Cx3cr1^{CreERT2}; Rosa^{YFP} mice at indicated time point post pulse (n = 5/group). (B) Gating strategy of intra-splenic MO. Dot plots are gated on viable single splenic cells. Intra-splenic MO are defined as Ly6C⁺ cells. (C) Flow cytometric analysis of YFP expression on intra-splenic MO and KCs within the same adult pulsed Csf1^{MerCreMer}; Rosa^{YFP} mice at indicated time point post intraperitoneal injection of 20mg/kg Clo (n = 4/group). (D) Flow-cytometric analysis of blood leukocytes and KCs from adult pulsed Csf1^{MerCreMer}; Rosa^{YFP} mice at 25-day post pulse (n = 5/group). (E) Flow-cytometric analysis of blood leukocytes and KCs from adult pulsed Csf1^{wt}; Rosa^{YFP} mice at 25-days post pulse (n = 5/group). (F), (G), (H), (I) Labeling index of intra-splenic MO and KCs at indicated time point post intraperitoneal injection of 20mg/kg Clo, analyzed in (C). *** P < 0.001. **Fig S6.** Flow-cytometric analysis of bone-marrow hematopoietic stem cells from C57BL/6 mice at indicated time point post intraperitoneal injection with 20gm/kg clodronate-liposomes (n = 5/group). **Fig S7.** Flow-cytometric analysis of blood hematopoietic stem cells (HSCs) from C57BL/6 mice at indicated time point post intraperitoneal injection with 20mg/kg Clo (n = 5/group). HSCs were defined as Lin^{neg}Sca-1⁺c-kit⁺CD34⁺CD135⁻ cells. **Fig S8.** Flow cytometric analysis of GFP liver non-parenchymal cells in kupffer cells-depleted mice revived GFP⁺ hematopoietic stem cells engraftment. **Fig S9.** Percent of GFP kupffer cells (KCs) from KC-depleted and purified

GFP⁺ hematopoietic stem cells engrafted, KC-depleted and purified GFP multipotent progenitors engrafted, or KC-depleted and purified GFP⁺ monocytic cells engrafted C57BL/6 mice at 90-day post-engraftment. Values are the means \pm SEM from 6 samples. ****P* < 0.001 between groups by ANOVA. **Fig S10.** Gating strategies of kupffer cells (KCs), bone marrow-derived mononuclear phagocytic system cells, macrophages, and blood leukocytes. A Gating strategy of non-parenchymal liver cells (NPCs). Dot plots are gated on total liver NPCs, 7-AAD⁺ dead cells, and doublets were excluded from the analysis and sorting. B Gating strategy of KCs. Dot plots are gated on viable single liver NPCs. KCs are defined as F4/80⁺, CD45⁺ C, CD11b⁺ D, and Ly6C⁻ E cells. F Gating strategy of bone marrow hematopoietic stem cells. 7-AAD⁺ dead cells and doublets were excluded from the analysis and sorting. Dot plots are gated on all bone marrow cells, then on Lineage-cells, then on Sca-1⁺ and c-kit⁺ cells, and finally on CD34⁻ CD135⁻ cells. Hematopoietic stem cells are defined as CD34⁻ and CD135⁻ CD48⁻ CD150⁻ LSK cells. LT-HSC is defined CD34⁻ and CD135⁻ CD48⁻ CD150⁻ LSK cells, ST-HSC is defined as CD34⁺ and CD135⁻ CD48⁻ CD150⁺ LSK cells, MMP2 is defined as CD135⁻ CD34⁻ CD150⁺ CD48⁺ LSK cells, MMP3 is defined as CD135⁻ CD34⁺ CD150⁻ CD48⁻, MMP4 is defined as CD135⁺ CD34⁺ CD150⁻ CD48⁺ LSK cells. G Gating strategy of bone marrow monocytic progenitors. H Gating strategy of bone marrow macrophages cells. I Gating strategy of blood B cells. J Gating strategy of blood T cells. K Gating strategy of blood monocytic cells. Dot plots are gated on blood cells in the monocyte region. Monocytic cells is defined as CD115⁺ cells. M Gating strategy of blood neutrophilia granulocyte.

Acknowledgements

We are grateful to W. Liu and other members of the Beijing center excellence, Becton-Dickinson Biosciences, for flow cytometry technical assistance.

Author contributions

XF designed the study, performed most of the experiments, analyzed the data, and wrote the manuscript. PL, XHC, HY, DZ, and HDW performed the fate-mapping experiments. PW, WRL, and FYC performed the PCR analysis. SZY and BL helped design the fate-mapping experiments. YJ designed most of the experiments and revised the manuscript. JDJ and BL helped revise the manuscript. YJ, JDJ, and FCH supervised the study. All authors have read and approved the manuscript.

Funding

This work was partially supported by National Key R&D Program of China (Nos. 2020YFE0202200, 2021YFA1301601, and 2018YFA0507502), the National Natural Science Foundation of China (Nos. 92168207, 82090051, 82273243, 81770581, and 81770598), Beijing Science and Technology Project (Nos. Z161100002616036 and Z15111000160000), Open Project Program of the State Key Laboratory of Proteomics (Nos. SKLP-K201801, SKLP-K201901, SKLP-O201902, SKLP-O202001, and SKLP-O201509), the China Postdoctoral Science Foundation (2014M552634), and Chinese Academy of Medical Sciences Innovation Fund for Medical Sciences (2019-12M-5-063).

Availability of data and materials

All data generated or analyzed during this study that are not included in this published article and its supplementary information files are available from the corresponding authors on reasonable request.

Declarations

Ethics approval and consent to participate

All experimental protocols were approved by the Institutional Animal Care and Use Committee of National Center of Protein Sciences (Beijing). Title of the approved project: The Exploration for Cellular Origin of Repopulating Kupffer Cells. The ethics approval (IACUC-20151221-12) was obtained on January 1, 2016. The care and use of animals were performed strictly following the regulations on the management of experimental animals.

Consent for publication

Not applicable.

Competing interests

The authors declare no competing interests.

Received: 6 December 2022 Accepted: 13 November 2023

Published online: 10 December 2023

References

- Krenkel O, Tacke F. Liver macrophages in tissue homeostasis and disease. *Nat Rev Immunol.* 2017;17(5):306–21.
- Davies LC, Taylor PR. Tissue-resident macrophages: then and now. *Immunology.* 2015;144(4):541–8.
- Perdiguero EG, Geissmann F. The development and maintenance of resident macrophages. *Nat Immunol.* 2016;17(1):2–8.
- McGrath KE, Frame JM, Palis J. Early hematopoiesis and macrophage development. *Semin Immunol.* 2015;27(6):379–87.
- Hashimoto D, Chow A, Noizat C, Teo P, Beasley MB, Leboeuf M, et al. Tissue-resident macrophages self-maintain locally throughout adult life with minimal contribution from circulating monocytes. *Immunity.* 2013;38(4):792–804.
- Yamamoto T, Naito M, Moriyama H, Umezumi H, Matsuo H, Kiwada H, et al. Repopulation of murine Kupffer cells after intravenous administration of liposome-encapsulated dichloromethylene diphosphonate. *Am J Pathol.* 1996;149(4):1271–86.
- Gentek R, Molawi K, Sieweke MH. Tissue macrophage identity and self-renewal. *Immunol Rev.* 2014;262(1):56–73.
- Scott CL, Zheng F, De Baetselier P, Saeyens Y, De Prijck S, Lippens S, et al. Bone marrow-derived monocytes give rise to self-renewing and fully differentiated Kupffer cells. *Nat Commun.* 2016;7:10321.
- Blériot C, Dupuis T, Jouvion G, Eberl G, Disson O, Lecuit M. Liver-resident macrophage necroptosis orchestrates type 1 microbicidal inflammation and type-2-mediated tissue repair during bacterial infection. *Immunity.* 2015;42(1):145–58.
- Aziz A, Soucie E, Sarrazin S, Sieweke MH. MafB/c-Maf deficiency enables self-renewal of differentiated functional macrophages. *Science.* 2009;326(5954):867–71.
- Yamada M, Naito M, Takahashi K. Kupffer cell proliferation and glucan-induced granuloma formation in mice depleted of blood monocytes by strontium-89. *J Leukoc Biol.* 1990;47(3):195–205.
- Klein I, Cornejo JC, Polakos NK, John B, Wuensch SA, Topham DJ, et al. Kupffer cell heterogeneity: functional properties of bone marrow derived and sessile hepatic macrophages. *Blood.* 2007;110(12):4077–85.
- Wynn TA, Chawla A, Pollard JW. Macrophage biology in development, homeostasis and disease. *Nature.* 2013;496(7446):445–55.
- Golde WT, Gollobin P, Rodriguez LL. A rapid, simple, and humane method for submandibular bleeding of mice using a lancet. *Lab Anim (NY).* 2005;34(9):39–43.
- Davis BK. Isolation, culture, and functional evaluation of bone marrow-derived macrophages. *Methods Mol Biol.* 2013;1031:27–35.
- Xu F, Zhen P, Zheng Y, Lijuan F, Aiting Y, Min C, et al. Preparation of Kupffer cell enriched non-parenchymal liver cells with high yield and reduced damage of surface markers by a modified method for flow cytometry. *Cell Biol Int.* 2013;37(4):284–91.
- Epelman S, Lavine KJ, Beaudin AE, Sojka DK, Carrero JA, Calderon B, et al. Embryonic and adult-derived resident cardiac macrophages are maintained through distinct mechanisms at steady state and during inflammation. *Immunity.* 2014;40(1):91–104.
- DeFalco T, Bhattacharya I, Williams AV, Sams DM, Capel B. Yolk-sac-derived macrophages regulate fetal testis vascularization and morphogenesis. *Proc Natl Acad Sci U S A.* 2014;111(23):E2384–93.
- Yanger K, Knigin D, Zong Y, Maggs L, Gu G, Akiyama H, et al. Adult hepatocytes are generated by self-duplication rather than stem cell differentiation. *Cell Stem Cell.* 2014;15(3):340–9.
- Liu X, Zhan Z, Li D, Xu L, Ma F, Zhang P, et al. Intracellular MHC class II molecules promote TLR-triggered innate immune responses by maintaining activation of the kinase Btk. *Nat Immunol.* 2011;12(5):416–24.
- Kinoshita M, Uchida T, Sato A, Nakashima M, Nakashima H, Shono S, et al. Characterization of two F4/80-positive Kupffer cell subsets by their function and phenotype in mice. *J Hepatol.* 2010;53(5):903–10.

22. Waskow C, Madan V, Bartels S, Costa C, Blasig R, Rodewald HR. Hematopoietic stem cell transplantation without irradiation. *Nat Methods*. 2009;6(4):267–9.
23. Yona S, Kim KW, Wolf Y, Mildner A, Varol D, Breker M, et al. Fate mapping reveals origins and dynamics of monocytes and tissue macrophages under homeostasis. *Immunity*. 2013;38(1):79–91.
24. Tarlow BD, Finegold MJ, Grompe M. Clonal tracing of Sox9+ liver progenitors in mouse oval cell injury. *Hepatology*. 2014;60(1):278–89.
25. DeGregorio MW, Coronado E, Osborne CK. Tumor and serum tamoxifen concentrations in the athymic nude mouse. *Cancer Chemother Pharmacol*. 1989;23(2):68–70.
26. Coombes JD, Swiderska-Syn M, Dollé L, Reid D, Eksteen B, Claridge L, et al. Osteopontin neutralisation abrogates the liver progenitor cell response and fibrogenesis in mice. *Gut*. 2015;64(7):1120–31.
27. Gazit R, Mandal PK, Ebina W, Ben-Zvi A, Nombela-Arrieta C, Silberstein LE, et al. Fgd5 identifies hematopoietic stem cells in the murine bone marrow. *J Exp Med*. 2014;211(7):1315–31.
28. Busch K, Klapproth K, Barile M, Flossdorf M, Holland-Letz T, Schlenner SM, et al. Fundamental properties of unperturbed haematopoiesis from stem cells in vivo. *Nature*. 2015;518(7540):542–6.
29. Breunig JJ, Arellano JI, Macklis JD, Rakic P. Everything that glitters isn't gold: a critical review of postnatal neural precursor analyses. *Cell Stem Cell*. 2007;1(6):612–27.
30. Dor Y, Brown J, Martinez OI, Melton DA. Adult pancreatic beta-cells are formed by self-duplication rather than stem-cell differentiation. *Nature*. 2004;429(6987):41–6.
31. Westermark L, Fahlgren A, Fällman M. Immune response to diphtheria toxin-mediated depletion complicates the use of the CD11c-DTR(tg) model for studies of bacterial gastrointestinal infections. *Microb Pathog*. 2012;53(3–4):154–61.
32. Roberts LM, Ledvina HE, Tuladhar S, Rana D, Steele SP, Sempowski GD, et al. Depletion of alveolar macrophages in CD11c diphtheria toxin receptor mice produces an inflammatory response. *Immun Inflamm Dis*. 2015;3(2):71–81.
33. Männ L, Kochupurakkal N, Martin C, Verjans E, Klingberg A, Sody S, et al. CD11c.DTR mice develop a fatal fulminant myocarditis after local or systemic treatment with diphtheria toxin. *Eur J Immunol*. 2016;46(8):2028–42.
34. Morinaga H, Mayoral R, Heinrichsdorff J, Osborn O, Franck N, Hah N, et al. Characterization of distinct subpopulations of hepatic macrophages in HFD/obese mice. *Diabetes*. 2015;64(4):1120–30.
35. Gomez Perdiguero E, Klapproth K, Schulz C, Busch K, Azzoni E, Crozet L, et al. Tissue-resident macrophages originate from yolk-sac-derived erythro-myeloid progenitors. *Nature*. 2015;518(7540):547–51.
36. Ved N, Curran A, Ashcroft FM, Sparrow DB. Tamoxifen administration in pregnant mice can be deleterious to both mother and embryo. *Lab Anim*. 2019;53(6):630–3.
37. Chow A, Brown BD, Merad M. Studying the mononuclear phagocyte system in the molecular age. *Nat Rev Immunol*. 2011;11(11):788–98.
38. Williams KL, Broadbridge CL. Potency of naltrexone to reduce ethanol self-administration in rats is greater for subcutaneous versus intraperitoneal injection. *Alcohol*. 2009;43(2):119–26.
39. Chow A, Lucas D, Hidalgo A, Méndez-Ferrer S, Hashimoto D, Scheiermann C, et al. Bone marrow CD169+ macrophages promote the retention of hematopoietic stem and progenitor cells in the mesenchymal stem cell niche. *J Exp Med*. 2011;208(2):261–71.

Publisher's Note

Springer Nature remains neutral with regard to jurisdictional claims in published maps and institutional affiliations.

Ready to submit your research? Choose BMC and benefit from:

- fast, convenient online submission
- thorough peer review by experienced researchers in your field
- rapid publication on acceptance
- support for research data, including large and complex data types
- gold Open Access which fosters wider collaboration and increased citations
- maximum visibility for your research: over 100M website views per year

At BMC, research is always in progress.

Learn more biomedcentral.com/submissions

